Published in final edited form as:
Brain Behav Immun. 2007 January ; 21(1): 100–111. doi:10.1016/j.bbi.2006.05.001.

Distribution of ICAM-1 immunoreactivity during aging in the human orbitofrontal cortex

Jose Javier Miguel-Hidalgo[a,*], **Sorcha Nithuairisg**[a], **Craig Stockmeier**[a,b], and **Grazyna Rajkowska**[a]

[a] Department of Psychiatry and Human Behavior, University of Mississippi Medical Center, Jackson, MS 39216, USA

[b] Department of Psychiatry, Case Western Reserve University, Cleveland, OH 44106, USA

Abstract

Neurological and psychiatric alterations during aging are associated with increased cerebrovascular disturbances and inflammatory markers such as Intercellular Adhesion Molecule-1 (ICAM-1). We investigated whether the distribution of ICAM-1 immunoreactivity (ICAM-1-I) in histological sections from the left orbitofrontal cortex (ORB) was altered during normal aging. Postmortem tissue from the ORB of nine younger (27–54 years old) and 10 older (60–86) human subjects was collected. Cryostat sections were immunostained only with antibodies to ICAM-1 or together with an antibody to glial fibrillary acidic protein (GFAP). The total area fraction of ICAM-1-I, and the fraction of vascular and extravascular ICAM-1-I were quantified in the gray matter. Furthermore, we examined the association of extravascular ICAM-1-I to GFAP immunoreactive (GFAP-IR) astrocytes. In all subjects, brain blood vessels were similarly ICAM-1 immunoreactive, and in some subjects there was a variable number of extravascular patches of ICAM-1-I. The area fraction of ICAM-1-I was 120% higher ($p < .0001$) in the old subjects than in the young subjects. This increase localized mostly to the extravascular ICAM-1-I in register with GFAP-IR astrocytes. A much smaller, also age-dependent increase occurred in vascular ICAM-1-I. Our results indicate a dramatic increase in extravascular ICAM-1-I associated to GFAP-IR astrocytes in the ORB in normal aging. This increase may contribute to an enhanced risk for brain inflammatory processes during aging, although a role of extravascular ICAM-1 as a barrier to further inflammation cannot be ruled out.

Keywords

Neocortex; Astrocytes; GFAP; Vasculature; Inflammation; Postmortem

1. Introduction

The Intercellular Cell Adhesion Molecule 1 (ICAM-1) is expressed in vascular endothelial cells, immune cells and glial cells of the nervous system (Lee and Benveniste, 1999). In blood vessels, ICAM-1 supports cell adhesion interactions for leukocyte extravasation (Springer, 1994, 1995) and is up-regulated in inflammatory processes (Cannella and Raine, 1995; Dopp et al., 1994). In endothelial cells residing in white and gray matter of the human forebrain, ICAM-1 is expressed since early in development (Lee and Benveniste, 1999). Astrocytes and microglia also express ICAM-1 when cultured, and after brain trauma (Bell and Perry, 1995). ICAM-1 is also increased in age-related neurodegenerative diseases

* Corresponding author. Fax: +1 601 984 5899. jmiguel-hidalgo@psychiatry.umsmed.edu (J.J. Miguel-Hidalgo).

(Akiyama et al., 1993). Accordingly, in Alzheimer's disease, besides brain vasculature, ICAM-1 also localizes to amyloid plaques, forming extravascular aggregates (Akiyama et al., 1993; Verbeek et al., 1994). These ICAM-1 immunoreactive aggregates seem mostly absent in non-demented control subjects, even in presence of normal vascular ICAM-1 immunoreactivity (Dalmau et al., 1997; Lee and Benveniste, 1999). However, it is still unclear whether age-related changes of extravascular ICAM-1immunoreactivity, possibly in astrocytes, occur in the brain of normal, non-demented subjects.

Inflammatory processes in the brain increase with aging (Bodles and Barger, 2004; Cunningham et al., 2002; Forsey et al., 2003; Hellerstein, 1989; Kletsas et al., 2004; Miles et al., 2001), and increases observed in neurodegenerative disorders could be age-related. In animal models of brain injury, mRNA levels for ICAM-1 and inflammatory cytokines increase more in old than in young rats (Kyrkanides et al., 2001), in parallel with increased immunostaining of glial fibrillary acidic protein (GFAP) in astrocytes. Furthermore, in human subjects, there seems to be an age-related increase in astrocytic GFAP immunoreactivity in the cerebral cortex (Miguel-Hidalgo et al., 2000; Nichols et al., 1993; Prolla and Mattson, 2001; Si et al., 2004; Sykova et al., 1998) that might be paralleled by changes in key inflammatory molecules, particularly ICAM-1. In fact, astrocytes express ICAM-1 immunoreactivity in vitro and in vivo following brain damage (Aloisi et al., 1992; Kim, 1996; Kraus et al., 1992; Lee and Benveniste, 1999; Nordal and Wong, 2004; Olschowka et al., 1997; Shrikant et al., 1995; Weber et al., 1994).

The present study assessed whether two groups of non-psychiatric, non-demented normal subjects separated by age (a younger group with subjects 27–54, and an older group with subjects 60–86 years of age) could also be sorted on the basis of their vascular and extravascular ICAM-1 immunoreactivity in the gray matter of the cytoarchitectonically defined area 47 of the orbitofrontal cortex. We divided subjects into younger and older because previous research of ICAM-1 immunoreactivity in the late-life brain of normal controls and subjects with major depression considered subjects 60 years old and above as older (Thomas et al., 2000). In addition, studies of expression of the astrocytic protein GFAP or its mRNA have suggested that around the age of 60 and later the expression of GFAP increases significantly in the human brain (Nichols et al., 1993; David et al., 1997). Several brain neuroimaging studies also consider 60 years old as a cutoff for studying elderly patients (Lai et al., 2000; Steffens et al., 2003; Taylor et al., 2004). Area 47 was targeted because of its propensity to age-related alterations in neuronal activity (Lamar et al., 2004) and age-related volume reductions (Tisserand et al., 2002), which are particularly prominent in subjects with psychiatric (Rajkowska et al., 2005, 1999; Shenton et al., 2001; Taylor et al., 2003) and neurodegenerative (Freedman, 1990; Freedman et al., 1998) disorders. We also ascertained whether putative changes in ICAM-1 immunoreactivity are in spatial register with GFAP-IR astrocytes.

2. Methods

Brain tissues were obtained at autopsy at the Cuyahoga County Coroner's Office, Cleveland, OH. An ethical protocol approved by the Institutional Review Board of the University Hospitals of Cleveland was used and informed written consent was obtained from the next-of-kin for all subjects. Brain tissue was selected with a postmortem delay of less than 32 h, and only from subjects that underwent sudden death, without prolonged agonal state. Demographic features and cause of death for the subjects are listed in Table 1. Blood and urine samples from all subjects were examined by the toxicology laboratory of the coroner's office for the presence of substances of abuse or psychotropic medications. The toxicology screen for medications and substances of abuse includes classes of medications such as antidepressant and antipsychotic drugs, antiepileptic drugs, barbiturates, benzodiazepines,

sympathomimetic amines, ethanol, cocaine and its metabolites, opiates, phencyclidine and cannabinoids. Toxicological screen did not detect blood ethanol in any of the subjects. One subject had caffeine and one subjects presented propoxyphene and oxycodone. The remaining subjects were negative for all medications or substances tested.

Retrospective, informant-based psychiatric assessments were performed for all subjects, as previously described (Rajkowska et al., 1999; Stockmeier et al., 1998, 2002). For the purpose of this study, the goal was to examine tissue from subjects identified as not meeting DSM-IV diagnostic criteria for a major mental illness. By definition, these subjects are herein referred to as normal control subjects. See Table 1 for information on the subjects. A trained interviewer administered one of two structured clinical interviews to next-of-kin of subjects in the study. Diagnoses for Axis I disorders were assessed independently by a clinical psychologist and a psychiatrist, and consensus diagnosis was reached in conference, using all available information from the knowledgeable informants, the coroner's office, and previous hospitalizations and doctors' records. Kelly and Mann (1996) have validated the use of the so-called psychiatric autopsy by demonstrating good agreement between informant-based retrospective psychiatric assessments of deceased subjects and chart diagnoses generated by clinicians treating the same subjects before death.

The Schedule for Affective Disorders and Schizophrenia: lifetime version (SADS-L) was administered to knowledgeable next-of-kin of six of the subjects (Spitzer and Endicott, 1978). The presence or absence of an Axis I psychiatric disorder was determined using criteria from the *Diagnostic and Statistic Manual of Mental Disorders–Revised* (DSMIII-R; American Psychiatric Association, 1987). With the publication of The Structured Clinical Interview for DSM-IV Psychiatric Disorders (SCID), the clinical interview process was modified to use this questionnaire for the remaining 13 subjects (First et al., 1996). The clinical interviews, designed for administration to live subjects, were modified such that questions were asked about the deceased to a knowledgeable informant. Responses from the six subjects evaluated with the SADS-L were also recorded using the SCID, and DSM-IV criteria were also used in assessing these subjects, as previously described (Stockmeier et al., 1998). Within the last 2 weeks of life, or ever during their lifetimes, these subjects did not meet clinical criteria for an Axis I disorder by either the DSM-IIIR or DSM-IV guidelines. Five subjects in the younger group and six in the older group were non-smokers, three in the younger group and two in the older were active smokers, and two in each group were not smokers at the time of death but had a history of smoking several years before.

Subjects were excluded if there was any medical history or evidence at autopsy of head trauma, neurological or neurodegenerative disease, a psychoactive substance use disorder, or Axis I psychiatric illness. Histological sections of prefrontal cortex, hippocampus, and anterior temporal cortex were processed for routine H and E staining and immunohistochemically for β-amyloid and a neuropathologist did not detect any evidence of infarcts, demyelinating diseases, atrophy or heterotopia. No neuropathology was detected consistent with Alzheimer's disease.

Further details about the diagnostic procedures and methods for collecting information on human subjects are provided elsewhere (Rajkowska et al., 1999; Stockmeier et al., 2002).

2.1. Tissue sampling

The tissue samples were obtained from the left prefrontal cortex of 19 subjects without diagnosis of any psychiatric or neurodegenerative disorders (Table 1). The subjects were divided into two age groups. One younger group included subjects with less than 60 years of age at the time of death (range, 27–54 years; 5 male, 4 female) and an older group subjects with 60 or more years of age at the time of death (range, 60–86; 6 male, 4 female). Upon

autopsy, slabs of the frontal lobe were immediately frozen in isopentane and stored at −80 °C until sectioning. There was no significant difference between younger and older subjects in the freezer storage time (older, 84.1 ± 29.3 months; younger, 72.22 ± 23.9), in postmortem delay (older, 22.4 ± 4.2; younger, 20.6 ± 6.4 h) or in brain tissue pH (older, 6.73 ± 0.15; younger, 6.66 ± 0.36). Morphometric parameters of immunoreactive structures were measured in the rostral part of Brodmann's area 47 that covers the medial wall of the medial orbital sulcus in the left orbitofrontal cortex. Previously established cytoarchitectonic criteria for area 47 (Hof et al., 1995;Rajkowska et al., 1999) were used to select the cortical region of interest for the present study.

Frozen slabs of about 1 cm in thickness containing the lateral orbitofrontal brain region were cut into 20 μm-thick sections. Sections were collected onto gelatin-coated slides, and immediately vacuum dried and stored at −80 °C until immunohistochemical staining. An adjacent set of sections was Nissl-stained with Cresyl Violet to ensure the inclusion of cytoarchitectonic Brodmann's area 47. Three sections evenly spaced (400 μm) and adjacent to the Nissl- stained sections were chosen from each subject to be immunostained with antibodies to ICAM-1 and were used for measuring the area fraction of ICAM-1 immunoreactivity. Other adjacent sections were immunostained with fluorescent probes simultaneously to study the co-localization of both glial fibrillary acidic protein (GFAP) and ICAM-1 immunoreactivities in single sections.

3. Immunohistochemistry

Sections mounted on gelatin-coated slides were washed in cold PBS and fixed in 4% paraformaldehyde for 15 min. Subsequently, some sections were subjected to immunohistochemistry for ICAM-1 by first incubating them either with a primary sheep polyclonal antibody, (R and D Systems, Cat# AF720; dilution 1:750) or a primary mouse monoclonal antibody (Zymed Laboratories, Cat# 07-5403; dilution1:500) to ICAM-1 diluted in a 0.1 M Tris–HCl buffer (pH 7.6) containing 2% bovine serum albumin and 0.2% Triton-X 100 (incubation solution). Then they were washed and incubated with a biotinylated anti-sheep or anti-mouse antibody, washed again, and the binding of the antibody was visualized using the ABC kit (Vector Laboratories, Burlingham) and 3-3′-diaminobenzidine (DAB) enhanced with nickel ammonium sulfate as chromogen.

3.1. Immunofluorescence

In four randomly chosen subjects per group, sections adjacent to the ones used for staining of ICAM-1 alone were subjected to a double fluorescent immunolabeling procedure to detect in individual sections simultaneously ICAM-1 and the astrocytic marker GFAP. Each section was incubated overnight with the sheep polyclonal antibody (1:750) ICAM-1 and a mouse monoclonal antibody (1:1000) (Chemicon) to GFAP diluted in the incubation solution. After three washes in 0.1 M Tris–HCl buffer (pH 7.6), sections were incubated for 90 min with a mixture of a donkey anti-sheep antibody conjugated with the fluorochrome Cy2 (Jackson Immunochemicals) (1:500 dilution) and a donkey anti-mouse antibody conjugated to fluorochrome Cy5 (Jackson Immunochemicals) (1:500 dilution) and washed again before coverslipping.

In our experiments, omission of the primary or the secondary antibody resulted in the absence of immunostaining. Specific immunostaining was also suppressed by incubating the primary antibody with recombinant human ICAM-1 (R&D Systems Cat# ADP4) before incubating it with brain tissue sections. To reduce to a minimum the variability in the intensity of staining due to uncontrollable changes from experiment to experiment, each immunostaining experiment involved the same number of sections from both groups. Furthermore, in each experiment there were no less than four subjects per group. No

significant differences in non-specific background staining were detected between experiments.

3.2. Extent of ICAM-1 immunoreactivity

The total area covered by ICAM-1 immunoreactivity (strictly speaking, the two-dimensional projection of ICAM-1-immunoreactivity onto the microscope field) in sections of the orbitofrontal cortex was measured using sections stained with DAB. These measurements were directed to estimate: (1) the total area fraction of ICAM-1-immunoreactivity (ICAM-1-I); (2) the area fraction of ICAM-1-I in vessels; and (3) the area fraction of extravascular ICAM-1-I. Images of ICAM-1-I were obtained with a video camera attached to a bright-field microscope and analyzed with the Image-J (version 1.3) software from NIH as follows. Using a 4× objective, a region of interest (ROI) of fixed width (1530 μm) was centered over area 47, spanning all cortical layers. The microscope light was set to a constant intensity and the same filters and computer video settings were used for all sections. In each of the ROIs an image was obtained with the video camera and digitized into gray level images. Immunopositive structures were segmented by defining a background level of staining in an area of the section with no specific immunoreactivity (determined by comparing to non-specific staining in sections concurrently processed omitting the first antibody). Then, thresholding with a fixed level of 25 gray values over the background (gray levels were from 0 (brightest) to 255 (darkest)) was applied. By this procedure, a binary image of the area occupied by immunoreactivity was obtained. The area fraction occupied by ICAM-1-I in cortex was calculated by dividing the area covered with immunoreactivity by the total area occupied by the cortical layers in the outlined ROI, and expressed as a percentage. The average of three measurements obtained in the three samples per subject was considered the value of the area fraction for total ICAM-1-I in the orbitofrontal cortical tissue.

3.3. Estimation of the area fraction of vascular and extravascular ICAM-1-I

In all sections, ICAM-1-I was localized to structures with the morphology of medium or small blood vessels (1 and 2). Immunoreactivity in these structures was termed vascular ICAM-1-I. In addition, in some of the subjects, ICAM-1-I was also localized to considerably larger patches of immunoreactivity with rounded morphology (within which vessels could also sometimes be detected) (Figs. 1 and 2). Since these patches were localized clearly outside blood vessels, those patches were termed extravascular ICAM-1-I. Accordingly, we obtained an estimate of the area fraction of ICAM-1-I restricted to vessels by first outlining manually the patches of extravascular ICAM-1-I and excluding those patches from the original ROI. Next, this modified ROI was subjected to the same procedure for area fraction measurement as described above, and thus provided an estimate of the area fraction of ICAM-1-I in vessels. The fraction of total ICAM-1-I (that is the fraction relative to the area of the unmodified ROI) in the outlined patches was also computed. Assuming that inside the ICAM-1 immunoreactive (IR) patches the area fraction of vascular ICAM-1-I was the same as outside those patches, we also obtained an estimate of the area fraction of extravascular ICAM-1-I. In summary, the variables related to ICAM-1-I in the cortex that were examined in the present study were: area fraction of total ICAM-1-I, area fraction of vascular ICAM-1-I and area fraction of extravascular ICAM-1-I.

4. Co-labeling of GFAP and ICAM-1

As described above (see Section 3), in four subjects per group, immunoreactivity for ICAM-1 and for GFAP were examined in three individual sections per subject using simultaneously a mouse monoclonal antibody to GFAP and a sheep polyclonal antibody to ICAM-1. Secondary antibodies conjugated either to fluorochrome Cy2 (anti-sheep IgG antibody) or Cy5 (anti-mouse IgG antibody), were used to detect ICAM-1 or GFAP

respectively. Under the laser scanning confocal microscope (NIKON NC1) these fluorochromes are excited and emit fluorescence at non-overlapping wavelengths. Therefore, with the use of the appropriate filters, ICAM-1 and GFAP immunoreactivities were unequivocally differentiated because “bleeding” across different channels was prevented (Figs. 7 and 8). GFAP-immunoreactive (GFAP-IR) astrocytes are strongly stained whether individually or grouped in patches and sharply contrast with the background. To determine whether GFAP-IR astrocytes or groups of astrocytes were coextensive with extravascular ICAM-1-IR patches, sections with double labeling were examined by one of us (S.N.) at the confocal microscope blind to the group identification of the slides. The number of ICAM-1-IR patches in register with individual GFAP-IR astrocytes or groups of astrocytes, and those out of register with GFAP-IR astrocytes was recorded and these two variables used to determine whether ICAM-1-IR patches are spatially related to GFAP-IR astrocytes.

At all times, the microscope operator taking measurements was blinded to the age at the time of death and the group of the study subject.

4.1. Statistics

Means of the area fraction of ICAM-1-I in younger and older subjects were compared using analysis of covariance (ANCOVA) with freezer storage time, postmortem delay and brain tissue pH as co-variates. Correlation of the parameters of ICAM-1-I with age at the time of death was determined with a Pearson correlation matrix. In the graphs, summary data are reported as mean ± standard error of the mean. These data are shown without adjusting for the covariates.

5. Results

5.1. Qualitative observations in sections of ORB immunostained with DAB chromogen

In histological sections from the human prefrontal cortex ICAM-1 immunoreactivity (ICAM-1-I) can be found forming two different types of structures in the gray matter of area 47. In agreement with previous reports, ICAM-1-I was observed in small and medium-sized blood vessels of all subjects examined (Fig. 1). In addition to the ICAM-immunoreactive (ICAM-IR) blood vessels, sections from some brains contained considerably larger patches of extravascular ICAM-1-I with rounded or oval shapes, and a diffuse pattern of immunostaining (Figs. 1 and 2). These patches, when present, were localized to all cytoarchitectonic areas contained in the section of the ORB region (i.e., Brodmann's areas 47, 11, 12), although our quantitative analysis was centered on the medial part of the rostral area 47. Visual inspection of immunoreactive sections (after quantitative measurements were performed) revealed that in most subjects of the younger group extravascular ICAM-1-IR patches were absent or they were very scarce, even if vessels were intensely immunoreactive for ICAM-1. By contrast, in the older group most subjects carried abundant and much larger extravascular ICAM-1-IR patches in addition to the ICAM-1-I of blood vessels. To validate the above-described immunostaining obtained with the sheep polyclonal anti-ICAM-1 antibody we subjected sections (neighbor to those immunostained with the sheep antibody) from seven brains with different ages to a monoclonal anti-ICAM-1 antibody raised in mouse. In a pattern similar to that of the sheep polyclonal antibody, the mouse monoclonal antibody also labeled the blood vessels in all subjects (Fig. 3A and B). In addition, in the oldest subjects, patches of immunoreactivity were also conspicuous in the gray matter (Fig. 3B). Since the contrast between non-specific background and immunoreactive structures was better with the sheep antibody all the results and analysis reported below correspond to immunostaining with the polyclonal anti-ICAM-1 antibody made in sheep.

5.2. Area fraction of ICAM-1-IR structures

The total area fraction occupied by the ICAM-1-IR structures was examined quantitatively in sections immunostained with the chromogen DAB. ANCOVA using postmortem interval, brain pH, and time of tissue storage at −80 °C as co-variates, showed that the mean area fraction of ICAM-1-IR structures in area 47 of the ORB was significantly and dramatically higher on average by 120% in the group of the older subjects than in the group of younger subjects ($F(1, 14) = 28.61$, $p < .0001$) (Fig. 4).

Since ICAM-1-I is localized both to blood vessels and to diffuse extravascular patches, an estimate was made of the area fraction occupied by ICAM-1-IR vessels (Fig. 5A) and by extravascular ICAM-1-I (Fig. 5B). The area fraction of ICAM-1-I in vessels was larger by 29% in older than in younger subjects ($F(1, 14) = 9.71$, $p < .01$). In comparison, the area fraction of ICAM-1 in extravascular patches was dramatically increased 7.5-fold in older as compared to younger subjects ($F(1, 14) = 48.46$, $p < .00001$).

The observation of much higher area fraction of extravascular ICAM-1-I in the older as compared to the younger subjects prompted us to examine the correlation of ICAM-1-I area fraction with age after combining the subjects in both age groups (Fig. 6). There was only a slow linear increase of vascular ICAM-1-I with age (Fig. 6A) ($r^2 = .306$, $p < .02$). By contrast, the slope of the regression for the area fraction of extravascular ICAM-1-I was much steeper ($r^2 = .715$, $p < .0001$), with a dramatic increase mainly occurring between 60 and 70 years of age (Fig. 6B).

5.3. Fluorescent co-labeling of ICAM-1 and GFAP Immunoreactivities

Extravascular patches of ICAM-1-I form discrete regions within the gray matter, and those patches increase with age. The size and distribution of those patches is similar to the distribution of GFAP-IR astrocytes in the cortex of elderly subjects that we have observed in previous studies. In addition, GFAP immunoreactivity in cortical astrocytes increases with age in the brain of psychiatrically normal human subjects and in aging experimental animals (David et al., 1997; Nichols et al., 1993). Accordingly, we examined whether ICAM-1-IR extravascular patches were in register with GFAP-IR astrocytes or groups of astrocytes in the subjects included in the present study. Sections from eight subjects (4 older subjects and 4 younger subjects) were co-labeled for GFAP and ICAM-1 and the number of ICAM-1-IR patches co-extensive with GFAP-IR astrocytes within the gray matter of area 47 in three sections per brain were counted and expressed as a percentage of the total number of ICAM-1-IR patches detected. The vast majority (97%) of extravascular GFAP-IR patches were in register with GFAP-IR astrocytes in both groups (younger and older subjects) (Fig. 7).

When measuring the two-dimensional overlap of GFAP-IR processes with ICAM-1-IR structures in the four older subjects, we observed that between 75% and 82% of GFAP processes were unequivocally overlapped with ICAM-1 structures and in many instances the ICAM-1 immunoreactivity in single processes was confined within the limits of the GFAP immunoreactivity. The extravascular ICAM-1 immunoreactivity was not necessarily confined to GFAP-IR processes or cell bodies in older subjects, but diffuse ICAM-1-I also extended to the spaces in between astrocytic processes (Figs. 7 and 8). However, this diffuse immunostaining was interrupted at the distal ends of astrocytic GFAP-IR processes (Figs. 7 and 8A–C).

Due to the very low load of extravascular ICAM-1-I in the younger subjects most GFAP-IR structures in these subjects did not coexist with ICAM-1-I. However, extravascular ICAM-1-I associated with the rare, double-labeled astrocytes in these young subjects were invariably confined within the GFAP immunofluorescent astrocytic processes (Fig. 8D–F).

Common to both young and elderly subjects was that in many blood vessels, ICAM-1-I was not coextensive with the GFAP-IR astrocytic processes or GFAP-IR processes were adjacent but not coextensive with vascular ICAM-1-I (Fig. 8).

6. Discussion

The present results show that there is a dramatic increase in the area fraction of ICAM-1-I in the gray matter of the orbitofrontal cortex in normal subjects older than 60 years of age. This increase is mostly accounted for by the development of extravascular patches of ICAM-1-I. The extent of these patches was on average 7.5-fold larger in older than in younger subjects. These patches are in close spatial register with the processes of GFAP-IR astrocytes or confined within the limits of GFAP-IR astrocytic processes, suggesting that the increases in ICAM-1-I in the gray matter originate in astrocytes or that ICAM-1-I in the neuropil (extravascular ICAM-1-I) mainly occurs within the immediate vicinity of GFAP-I-IR astrocytic processes. Previous studies on the distribution of ICAM-1-I in the human brain have associated the existence of extravascular ICAM-1-IR patches to neurodegenerative disorders (Akiyama et al., 1993; Frohman et al., 1991; Verbeek et al., 1994). Akiyama et al. (1993) and Frohman et al. (1991) found that, besides being normally localized to brain capillaries, ICAM-1-I was partly associated with senile plaques in Alzheimer's disease. Interestingly, Akiyama et al. (1993) also found ICAM-1-IR patches in the postmortem brain of elderly subjects with other etiologically diverse neurodegenerative disorders like Pick's disease, amyotrophic lateral sclerosis or progressive supranuclear palsy (Akiyama et al., 1993), all of which progress with or are largely dependent on age. Another study (Verbeek et al., 1994) also described the presence of patches of ICAM-1-I as associated with senile plaques. The regions of ICAM-1-I in their samples, however, are considerably larger than the plaques themselves and the authors describe the presence of ICAM-1-I in diffuse deposits that were not labeled by anti-β-amyloid (Aβ) antibodies. They also reported that in control subjects (six older and two younger than 60 years of age) and in non-Alzheimer's dementia (AD) subjects, there were occasional deposits of ICAM-1-I in some instances. In the study of Akiyama et al. (1993) (Akiyama et al., 1993) some deposits of Aβ also appear to be devoid of ICAM-1-I and diffuse deposits of ICAM-1 were not exclusive to the diagnosis of AD but also present in other neurological conditions that worsen with age. In Verbeek's study however, there was no description of a possible correlation of the numbers of occasional ICAM-1-IR structures and age.

A possible limitation of the present study is that, since data on the subjects were coroner-based, cross-sectional and retrospectively recorded, we do not have prospective data of memory and other cognitive functions based on quantifiable tests. Thus it is not possible to study whether there is a correlation between the performance in those functions and the extent of ICAM-1 immunoreactivity. However, in our brain collection, information on the subjects is examined to determine if a psychiatric diagnosis (see Section 2 for details) is associated with a particular subject. Information on each subject is also screened and a neuropathological examination is performed to rule out diagnosis of neurological and neurodegenerative disease. Subjects are considered normal controls when there is no information or neuropathological data indicating of psychiatric or neurological disorders.

The apparently smaller extent of extravascular ICAM-1-I in elderly subjects by Verbeek et al. (1994) as compared to our findings might be due to several reasons. In Verbeek et al. (1994) sections subjected to immunohistochemistry had a thickness of 4 μm (5 × thinner than our sections) and used a peroxidase conjugated secondary antibody. In our study we used 20 μm-thick sections and a biotinylated secondary antibody and the ABC complex (which increases sensitivity of the immunostaining). Thus, it is possible that if the concentration of ICAM-1 in and around senile plaques is higher than in other deposits of

extravascular ICAM-1, non-plaque ICAM-1 immunoreactivity may have been confused with the background or not detected. Furthermore, in the present report, the number of control subjects in each of the age groups was considerably larger than that in Verbeek et al. (1994), which increased the ability of detecting age related changes and the power of the statistical tests applied. Since the postmortem delay in Verbeek et al. (1994) was shorter than in both groups of the present study it is also possible that longer postmortem delay tends to increase the amount of detectable extravascular ICAM-1-I related to astrocytes. However, if that was the only reason for detecting increased ICAM-1-I in the present study, that increase should have been of the same magnitude in young and old subjects. On the contrary, in the present study extravascular ICAM-1-I was still dramatically lower in the younger than in the older subjects even though postmortem delays were not significantly different between groups (see Table 1). In addition, in a study of ICAM-1-I in the prefrontal cortex of elderly subjects, postmortem delay periods were reported (Thomas et al., 2002) that were longer than in the present study, and ICAM-1-I was only described in blood vessels. However, these studies (41) were made with tissue with a long fixation time (about 10 years) and using paraffin embedding, while we used fresh frozen tissue that was stored at −80 °C for no more than 4 years. These facts clearly argue for a genuine dramatic increase in extravascular ICAM–1-I in older control subjects as compared to younger subjects.

I-CAM-1 is a protein that spans the cell membrane and has cytoplasmic, intramembranous and extracellular domains (Lee and Benveniste, 1999). Consequently ICAM-1 is normally detected bound to the membrane. However, soluble forms of the protein, mainly representing the extracellular N-terminal fragment of the protein have been detected in vivo and in vitro (Baraczka et al., 2001; Rothlein et al., 1991; Seth et al., 1991). In our immunohistochemical studies a large portion of non-vascular ICAM-1-I although always associated with the region of tissue reached by GFAP-IR processes, presents a diffuse pattern of distribution in the neuropil. This pattern suggests that there are forms of ICAM-1 that might be soluble and represent an important portion of the ICAM-1-I in the cortex of older subjects. The co-localization and proximity of ICAM-1-I to astrocytes processes suggests that increases in astroglial activation in the elderly may be related to increased synthesis and release in ICAM-1. This preferential relationship of ICAM-1 to astrocytes is consistent with the absence of co-labeling of microglial markers and patches of ICAM-1 immunoreactivity in the brain of Alzheimer's patients (Frohman et al., 1991). Age-related increases in the levels of GFAP and in the density of GFAP immunoreactive astrocytes actually have been reported in the human neocortex and other brains regions and they could be related to the dramatically increased ICAM-1-I in the elderly (Miguel-Hidalgo et al., 2000; Nichols et al., 1993; Prolla and Mattson, 2001; Si et al., 2004; Sykova et al., 1998) (David et al., 1997; Miguel-Hidalgo et al., 2000; Nichols et al., 1993). These increases occur even in the absence of cognitive deficits or neuropathological hallmarks of Alzheimer's disease (David et al., 1997).

Some researchers suggest that soluble ICAM-1 might compete for receptors of membrane bound ICAM-1 and effectively inhibit aging related increases in immune responses in the brain (Hailer et al., 1998). Such a role would be consistent with comparatively good cognitive performance detected in elderly subjects even when they have high levels of ICAM-1 (Elwan et al., 2003). A specific role for astrocyte-generated ICAM-1 as compared to ICAM-1 from endothelial cells is suggested by increases in soluble ICAM-1 in patients with traumatic brain injury and in a mouse model of traumatic brain injury (Otto et al., 2000), in which the production of soluble ICAM-1 was much higher in astrocytes than in endothelial cells.

Disruption of the blood brain barrier has been correlated with increases in inflammatory molecules including ICAM-1 (Dietrich, 2002; Lossinsky et al., 1995; Schnell et al., 1999).

Although blood brain barrier alterations during normal aging are very likely of much lower magnitude than in brain trauma, it is possible that they are sufficient to trigger increased ICAM-1 in astrocytes. Alternatively to a protective role suggested above, astrocyte-generated ICAM-1 might play a role in monocyte recruitment to the brain in aged individuals through the regulation of macrophage inflammatory proteins (MCPs) (Andjelkovic et al., 2000; Otto et al., 2002). This regulation would increase the probability of developing inflammatory processes. However, in Nissl- stained sections from the brains in the present study, we did not detect visually noticeable increases of cells in general or cells with leukocyte morphology around vessels. Additional experiments targeting macrophages and other leukocytes with specific markers should examine whether these cells co-occur with the diffuse patches of ICAM –1 immunoreactivity in the aging human brain.

In addition to an age-related increase in the area fraction of extravascular ICAM-1-I, we also observed a much more modest increase in the area fraction of ICAM-1-I in blood vessels, which is consistent with increased markers of inflammation observed by other researchers in blood vessels during aging (d'Alessio, 2004; Finch, 2005; Minamino et al., 2004).

A possible limitation to the generalization of our conclusions to all subjects undergoing normal aging is that the cause of death for most subjects in our study was related to cardiovascular factors, which are responsible for a high proportion of sudden deaths. Since inflammation has been related to cardiovascular disturbances an influence it could be argued that cardiovascular cause of death was related to increased ICAM-1 immunoreactivity. However, as shown in Table 1, a vascular cause of death in the younger subjects was as well represented as in the older subjects so that the differences in ICAM-1 immunoreactivity between these two groups of subjects would be rather due to other factors that change with age.

Increases of ICAM-1-I in brain vessels have been often related to different types of injury, and associated to the appearance of inflammatory processes (Dopp et al., 1994; Feuerstein et al., 1997; Olschowka et al., 1997; Whalen et al., 1998). Recent studies on the etiopathology of major depression in the elderly have also related increased vascular disturbances and inflammation to late-life depression (Alexopoulos et al., 1997; Krishnan and McDonald, 1995). More specifically, increases in the extent of ICAM-1-IR vessels have been reported in the brain of elderly subjects with depression as compared to control elderly subjects (Thomas et al., 2004, 2000). Interestingly, these reports, although using an antibody from the same source as in our study, do not mention the presence of extravascular patches of ICAM-1 immunoreactivity. Nevertheless, the results presented here suggest that, when characterizing ICAM-1 immunoreactivity in the human prefrontal cortex, the expression of extravascular ICAM-1-immunoreactive structures and its relationship to age should be taken into account, particularly when considering the close relationship of ICAM-1 immunoreactivity to astrocytes detected in our study. It remains to be elucidated whether vascular and extravascular ICAM-1-IR structures perform differential functions and what is the specific role of astrocytes in the age-related increase of extravascular ICAM-1 immunoreactivity in the prefrontal cortex.

Acknowledgments

The authors thankfully acknowledge the work of James C. Overholser, Ph.D., George Jurjus, M.D., and Lisa Konick in the establishment of retrospective psychiatric diagnoses. We also acknowledge the excellent assistance of the Cuyahoga County Coroner's Office, Cleveland, OH, and the cooperation and support of the next-of-kin of the deceased. We are grateful as well to Qingmei Shao for her skillful technical assistance in preparing histological specimens. Funding supported by NIH Grants: MH60451, MH63187 and RR17701.

References

Akiyama H, Kawamata T, Yamada T, Tooyama I, Ishii T, McGeer PL. Expression of intercellular adhesion molecule (ICAM)-1 by a subset of astrocytes in Alzheimer disease and some other degenerative neurological disorders. Acta Neuropathol (Berl). 1993; 85:628–634. [PubMed: 8337942]

Alexopoulos G, Meyers B, Young R, Campbell S, Silbersweig D, Charlson M. 'Vascular depression' hypothesis. Arch Gen Psychiatry. 1997; 54:915–922. [PubMed: 9337771]

Aloisi F, Borsellino G, Samoggia P, Testa U, Chelucci C, Russo G, Peschle C, Levi G. Astrocyte cultures from human embryonic brain: characterization and modulation of surface molecules by inflammatory cytokines. J Neurosci Res. 1992; 32:494–506. [PubMed: 1356158]

Andjelkovic AV, Kerkovich D, Pachter JS. Monocyte: astrocyte interactions regulate MCP-1 expression in both cell types. J Leukoc Biol. 2000; 68:545–552. [PubMed: 11037977]

Baraczka K, Nekam K, Pozsonyi T, Jakab L, Szongoth M, Sesztak M. Concentration of soluble adhesion molecules (sVCAM-1, sICAM-1 and sL-selectin) in the cerebrospinal fluid and serum of patients with multiple sclerosis and systemic lupus erythematosus with central nervous involvement. Neuroimmunomodulation. 2001; 9:49–54. [PubMed: 11435752]

Bell MD, Perry VH. Adhesion molecule expression on murine cerebral endothelium following the injection of a proinflammagen or during acute neuronal degeneration. J Neurocytol. 1995; 24:695–710. [PubMed: 7500124]

Bodles AM, Barger SW. Cytokines and the aging brain—what we don't know might help us. Trends Neurosci. 2004; 27:621–626. [PubMed: 15374674]

Cannella B, Raine CS. The adhesion molecule and cytokine profile of multiple sclerosis lesions. Ann Neurol. 1995; 37:424–435. [PubMed: 7536402]

Cunningham C, Konsman JP, Cartmell T. Cytokines and the ageing brain. Trends Neurosci. 2002; 25:546–547. [PubMed: 12392922]

Dalmau I, Vela JM, Gonzalez B, Castellano B. Expression of LFA-1alpha and ICAM-1 in the developing rat brain: a potential mechanism for the recruitment of microglial cell precursors. Brain Res Dev Brain Res. 1997; 103:163–170.

David JP, Ghozali F, Fallet-Bianco C, Wattez A, Delaine S, Boniface B, Di Menza C, Delacourte A. Glial reaction in the hippocampal formation is highly correlated with aging in human brain. Neurosci Lett. 1997; 235:53–56. [PubMed: 9389594]

Dietrich JB. The adhesion molecule ICAM-1 and its regulation in relation with the blood-brain barrier. J Neuroimmunol. 2002; 128:58–68. [PubMed: 12098511]

Dopp JM, Breneman SM, Olschowka JA. Expression of ICAM-1, VCAM-1, L-selectin, and leukosialin in the mouse central nervous system during the induction and remission stages of experimental allergic encephalomyelitis. J Neuroimmunol. 1994; 54:129–144. [PubMed: 7523443]

d'Alessio P. Aging and the endothelium. Exp Gerontol. 2004; 39:165–171. [PubMed: 15038389]

Elwan O, Madkour O, Elwan F, Mostafa M, Abbas Helmy A, Abdel-Naseer M, Abdel Shafy S, El Faiuomy N. Brain aging in normal Egyptians: cognition, education, personality, genetic and immunological study. J Neurol Sci. 2003; 211:15–22. [PubMed: 12767492]

Feuerstein GZ, Wang X, Barone FC. Inflammatory gene expression in cerebral ischemia and trauma. Potential new therapeutic targets. Ann N Y Acad Sci. 1997; 825:179–193. [PubMed: 9369986]

Finch CE. Developmental origins of aging in brain and blood vessels: an overview. Neurobiol Aging. 2005; 26:281–291. [PubMed: 15639305]

First, MB.; Spitzer, RL.; Gibbon, M.; Williams, JBW. Structured Clinical Interview for DSM-IV Axis I Disorders—patient edition (SCID-I/P, Version 2.0). Biometrics Research Department, New York State Psychiatric Institute; 1996.

Forsey RJ, Thompson JM, Ernerudh J, Hurst TL, Strindhall J, Johansson B, Nilsson BO, Wikby A. Plasma cytokine profiles in elderly humans. Mech Ageing Dev. 2003; 124:487–493. [PubMed: 12714257]

Freedman M. Object alternation and orbitofrontal system dysfunction in Alzheimer's and Parkinson's disease. Brain Cogn. 1990; 14:134–143. [PubMed: 2285509]

Freedman M, Black S, Ebert P, Binns M. Orbitofrontal function, object alternation and perseveration. Cereb Cortex. 1998; 8:18–27. [PubMed: 9510382]

Frohman EM, Frohman TC, Gupta S, de Fougerolles A, van den Noort S. Expression of intercellular adhesion molecule 1 (ICAM-1) in Alzheimer's disease. J Neurol Sci. 1991; 106:105–111. [PubMed: 1685745]

Hailer NP, Heppner FL, Haas D, Nitsch R. Astrocytic factors deactivate antigen presenting cells that invade the central nervous system. Brain Pathol. 1998; 8:459–474. [PubMed: 9669697]

Hellerstein MK. Aging, diet, and the acute-phase response to inflammation. Ann N Y Acad Sci. 1989; 561:178–195. [PubMed: 2500054]

Hof PR, Mufson EJ, Morrison JH. Human orbitofrontal cortex: cytoarchitecture and quantitative immunohistochemical parcellation. J Comp Neurol. 1995; 359:48–68. [PubMed: 8557847]

Kelly TM, Mann JJ. Validity of DSM-III-R diagnosis by psychological autopsy: a comparison with clinician ante-mortem diagnosis. Acta Psychiatr Scand. 1996; 94:337–343. [PubMed: 9124080]

Kim JS. Cytokines and adhesion molecules in stroke and related diseases. J Neurol Sci. 1996; 137:69–78. [PubMed: 8782158]

Kletsas D, Pratsinis H, Mariatos G, Zacharatos P, Gorgoulis VG. The proinflammatory phenotype of senescent cells: the p53-mediated ICAM-1 expression. Ann N Y Acad Sci. 2004; 1019:330–332. [PubMed: 15247038]

Kraus E, Schneider_Schaulies S, Miyasaka M, Tamatani T, Sedgwick J. Augmentation of major histocompatibility complex class I and ICAM-1 expression on glial cells following measles virus infection: evidence for the role of type-1 interferon. Eur J Immunol. 1992; 22:175–182. [PubMed: 1346110]

Krishnan K, McDonald W. Arteriosclerotic depression. Med Hypotheses. 1995; 44:111–115. [PubMed: 7596303]

Kyrkanides S, O_Banion MK, Whiteley PE, Daeschner JC, Olschowka JA. Enhanced glial activation and expression of specific CNS inflammation-related molecules in aged versus young rats following cortical stab injury. J Neuroimmunol. 2001; 119:269–277. [PubMed: 11585630]

Lai T, Payne ME, Byrum CE, Steffens DC, Krishnan KR. Reduction of orbital frontal cortex volume in geriatric depression. Biol Psychiatry. 2000; 48:971–975. [PubMed: 11082470]

Lamar M, Yousem DM, Resnick SM. Age differences in orbitofrontal activation: an fMRI investigation of delayed match and non-match to sample. Neuroimage. 2004; 21:1368–1376. [PubMed: 15050562]

Lee SJ, Benveniste EN. Adhesion molecule expression and regulation on cells of the central nervous system. J Neuroimmunol. 1999; 98:77–88. [PubMed: 10430040]

Lossinsky AS, Mossakowski MJ, Pluta R, Wisniewski HM. Intercellular adhesion molecule-1 (ICAM-1) upregulation in human brain tumors as an expression of increased blood-brain barrier permeability. Brain Pathol. 1995; 5:339–344. [PubMed: 8974619]

Miguel-Hidalgo JJ, Baucom C, Dilley G, Overholser JC, Meltzer HY, Stockmeier CA, Rajkowska G. GFAP-immunoreactivity in the prefrontal cortex distinguishes younger from older adults in major depressive disorder. Biol Psychiatry. 2000; 48:860–872.

Miles EA, Thies F, Wallace FA, Powell JR, Hurst TL, Newsholme EA, Calder PC. Influence of age and dietary fish oil on plasma soluble adhesion molecule concentrations. Clin Sci (Lond). 2001; 100:91–100. [PubMed: 11115423]

Minamino T, Miyauchi H, Yoshida T, Tateno K, Kunieda T, Komuro I. Vascular cell senescence and vascular aging. J Mol Cell Cardiol. 2004; 36:175–183. [PubMed: 14871544]

Nichols NR, Day JR, Laping NJ, Johnson SA, Finch CE. GFAP mRNA increases with age in rat and human brain. Neurobiol Aging. 1993; 14:421–429. [PubMed: 8247224]

Nordal RA, Wong CS. Intercellular adhesion molecule-1 and blood-spinal cord barrier disruption in central nervous system radiation injury. J Neuropathol Exp Neurol. 2004; 63:474–483. [PubMed: 15198126]

Olschowka JA, Kyrkanides S, Harvey BK, O'Banion MK, Williams JP, Rubin P, Hansen JT. ICAM-1 induction in the mouse CNS following irradiation. Brain Behav Immun. 1997; 11:273–285. [PubMed: 9512815]

Otto VI, Gloor SM, Frentzel S, Gilli U, Ammann E, Hein AE, Folkers G, Trentz O, Kossmann T, Morganti-Kossmann MC. The production of macrophage inflammatory protein-2 induced by soluble intercellular adhesion molecule-1 in mouse astrocytes is mediated by src tyrosine kinases and p42/44 mitogen-activated protein kinase. J Neurochem. 2002; 80:824–834. [PubMed: 11948246]

Otto VI, Heinzel-Pleines UE, Gloor SM, Trentz O, Kossmann T, Morganti-Kossmann MC. sICAM-1 and TNF-alpha induce MIP-2 with distinct kinetics in astrocytes and brain microvascular endothelial cells. J Neurosci Res. 2000; 60:733–742. [PubMed: 10861785]

Prolla TA, Mattson MP. Molecular mechanisms of brain aging and neurodegenerative disorders: lessons from dietary restriction. Trends Neurosci. 2001; 24:S21–S31. [PubMed: 11881742]

Rajkowska G, Miguel-Hidalgo JJ, Dubey P, Stockmeier CA, Krishnan RR. Prominent reduction in pyramidal neurons density in the orbitofrontal cortex of elderly depressed patients. Biol Psychiatry. 2005; 58:297–306. [PubMed: 15953590]

Rajkowska G, Miguel-Hidalgo JJ, Wei J, Dilley G, Pittman SD, Meltzer HY, Overholser JC, Roth BL, Stockmeier CA. Morphometric evidence for neuronal and glial prefrontal cell pathology in major depression. Biol Psychiatry. 1999; 45:1085–1098. [PubMed: 10331101]

Rothlein R, Mainolfi EA, Czajkowski M, Marlin SD. A form of circulating ICAM-1 in human serum. J Immunol. 1991; 147:3788–3793. [PubMed: 1682385]

Schnell L, Fearn S, Klassen H, Schwab ME, Perry VH. Acute inflammatory responses to mechanical lesions in the CNS: differences between brain and spinal cord. Eur J Neurosci. 1999; 11:3648–3658. [PubMed: 10564372]

Seth R, Raymond FD, Makgoba MW. Circulating ICAM-1 isoforms: diagnostic prospects for inflammatory and immune disorders. Lancet. 1991; 338:83–84. [PubMed: 1676471]

Shenton ME, Dickey CC, Frumin M, McCarley RW. A review of MRI findings in schizophrenia. Schizophr Res. 2001; 49:1–52. [PubMed: 11343862]

Shrikant P, Weber E, Jilling T, Benveniste EN. Intercellular adhesion molecule-1 gene expression by glial cells. Differential mechanisms of inhibition by IL-10 and IL-6. J Immunol. 1995; 155:1489–1501. [PubMed: 7636212]

Si X, Miguel-Hidalgo JJ, O'Dwyer G, Stockmeier CA, Rajkowska G. Age-dependent reductions in the level of glial fibrillary acidic protein in the prefrontal cortex in major depression. Neuropsychopharmacology. 2004; 29:2088–2096. [PubMed: 15238995]

Spitzer, RL.; Endicott, J. Schedule for affective disorders and schizophrenia (SADS). Third. New York State Psychiatric Institute; New York: 1978.

Springer TA. Traffic signals for lymphocyte recirculation and leukocyte emigration: the multistep paradigm. Cell. 1994; 76:301–314. [PubMed: 7507411]

Springer TA. Traffic signals on endothelium for lymphocyte recirculation and leukocyte emigration. Annu Rev Physiol. 1995; 57:827–872. [PubMed: 7778885]

Steffens DC, McQuoid DR, Welsh-Bohmer KA, Krishnan KR. Left orbital frontal cortex volume and performance on the benton visual retention test in older depressives and controls. Neuropsychopharmacology. 2003; 28:2179–2183. [PubMed: 14532909]

Stockmeier CA, Shapiro LA, Dilley GE, Kolli TN, Friedman L, Rajkowska G. Increase in serotonin-1A autoreceptors in the midbrain of suicide victims with major depression-postmortem evidence for decreased serotonin activity. J Neurosci. 1998; 18:7394–7401. [PubMed: 9736659]

Stockmeier CA, Shi X, Konick L, Overholser JC, Jurjus G, Meltzer HY, Friedman L, Blier P, Rajkowska G. Neurokinin-1 receptors are decreased in major depressive disorder. Neuroreport. 2002; 13:1223–1227. [PubMed: 12151774]

Sykova E, Mazel T, Simonova Z. Diffusion constraints and neuron-glia interaction during aging. Exp Gerontol. 1998; 33:837–851. [PubMed: 9951627]

Taylor WD, MacFall JR, Payne ME, McQuoid DR, Provenzale JM, Steffens DC, Krishnan KR. Late-life depression and microstructural abnormalities in dorsolateral prefrontal cortex white matter. Am J Psychiatry. 2004; 161:1293–1296. [PubMed: 15229065]

Taylor WD, Steffens DC, McQuoid DR, Payne ME, Lee SH, Lai TJ, Krishnan KR. Smaller orbital frontal cortex volumes associated with functional disability in depressed elders. Biol Psychiatry. 2003; 53:144–149. [PubMed: 12547470]

Thomas AJ, Davis S, Ferrier IN, Kalaria RN, O'Brien JT. Elevation of cell adhesion molecule immunoreactivity in the anterior cingulate cortex in bipolar disorder. Biol Psychiatry. 2004; 55:652–655. [PubMed: 15013836]

Thomas AJ, Ferrier IN, Kalaria RN, Davis S, O'Brien JT. Cell adhesion molecule expression in the dorsolateral prefrontal cortex and anterior cingulate cortex in major depression in the elderly. Br J Psychiatry. 2002; 181:129–134. [PubMed: 12151283]

Thomas AJ, Ferrier IN, Kalaria RN, Woodward SA, Ballard C, Oakley A, Perry RH, O'Brien JT. Elevation in late-life depression of intercellular adhesion molecule-1 expression in the dorsolateral prefrontal cortex. Am J Psychiatry. 2000; 157:1682–1684. [PubMed: 11007725]

Tisserand DJ, Pruessner JC, Sanz Arigita EJ, van Boxtel MP, Evans AC, Jolles J, Uylings HB. Regional frontal cortical volumes decrease differentially in aging: an MRI study to compare volumetric approaches and voxel-based morphometry. Neuroimage. 2002; 17:657–669. [PubMed: 12377141]

Verbeek MM, Otte-Holler I, Westphal JR, Wesseling P, Ruiter DJ, de Waal RM. Accumulation of intercellular adhesion molecule-1 in senile plaques in brain tissue of patients with Alzheimer's disease. Am J Pathol. 1994; 144:104–116. [PubMed: 7904796]

Weber F, Meinl E, Aloisi F, Nevinny_Stickel C, Albert E, Wekerle H, Hohlfeld R. Human astrocytes are only partially competent antigen presenting cells. Possible implications for lesion development in multiple sclerosis. Brain. 1994; 117:59–69. [PubMed: 7511974]

Whalen MJ, Carlos TM, Kochanek PM, Wisniewski SR, Bell MJ, Carcillo JA, Clark RS, DeKosky ST, Adelson PD. Soluble adhesion molecules in CSF are increased in children with severe head injury. J Neurotrauma. 1998; 15:777–787. [PubMed: 9814634]

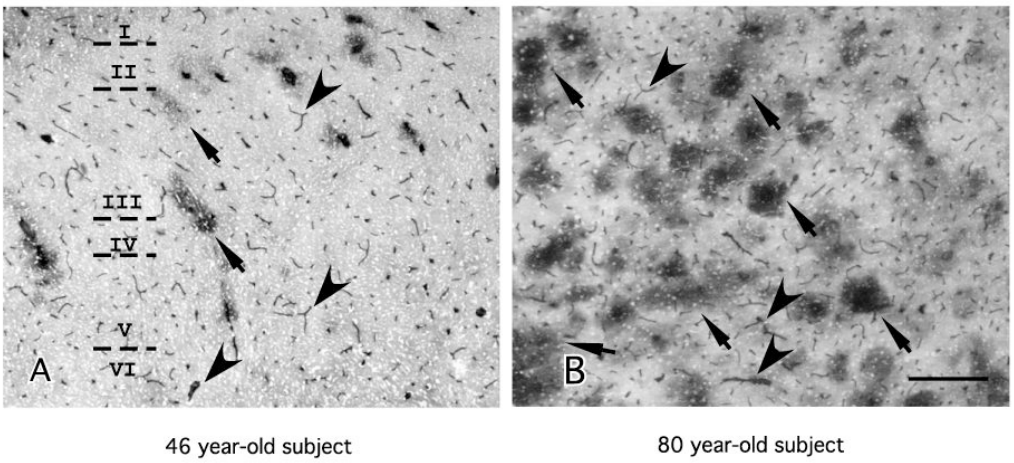

Fig. 1.

Low power micrographs of ICAM-1 immunoreactivity (sheep polyclonal antibody) encompassing all cortical layers (I–VI) in area 47 of two male human subjects of different age. (A) 46 years old, male; (B) 80 years old, male. Note that in both micrographs small and medium blood vessels are ICAM-1-IR (arrowheads). In addition, in the oldest subject (B) there are many large, round patches of diffuse ICAM-1-IR (arrows) that are much less abundant in the 46-year-old subject. Calibration bar, 250 μm.

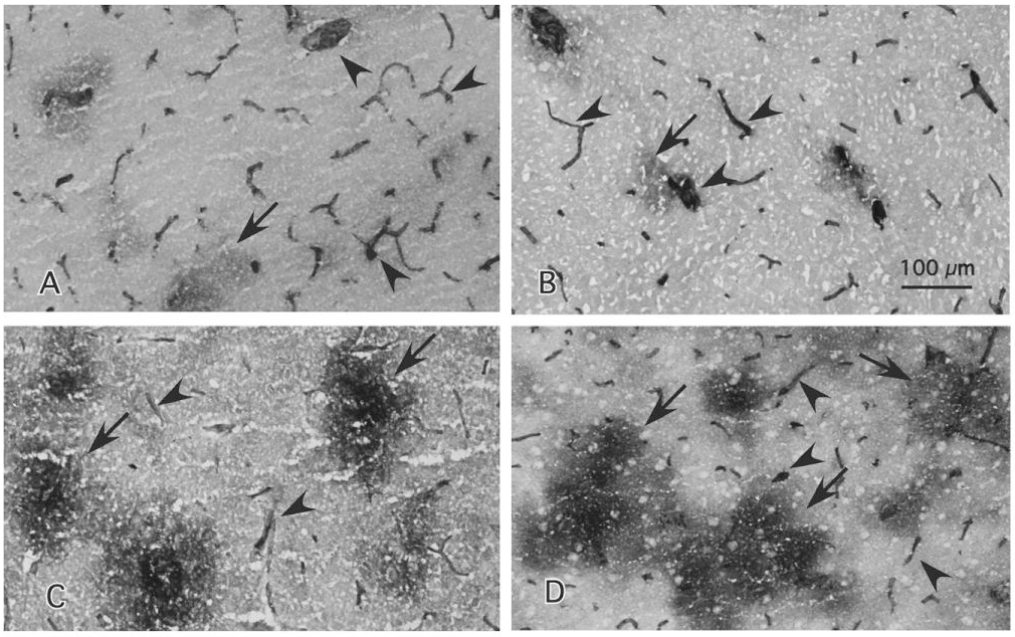

Fig. 2.

High power micrographs of immunostaining with the sheep polyclonal antibody to ICAM-1 taken from layer III of cortical area 47. The top panels correspond to younger male (A) and a female (B) subjects with ages 43 and 46 at the time of death, respectively. The bottom panels correspond to older male (C) and female (D) subjects with ages 77 and 80, respectively. Arrows point to the diffuse patches composed of extravascular ICAM-1 immunoreactivity as defined in the Section 2. Arrowheads denote immunoreactive vessels. Calibration bar, 100 μm.

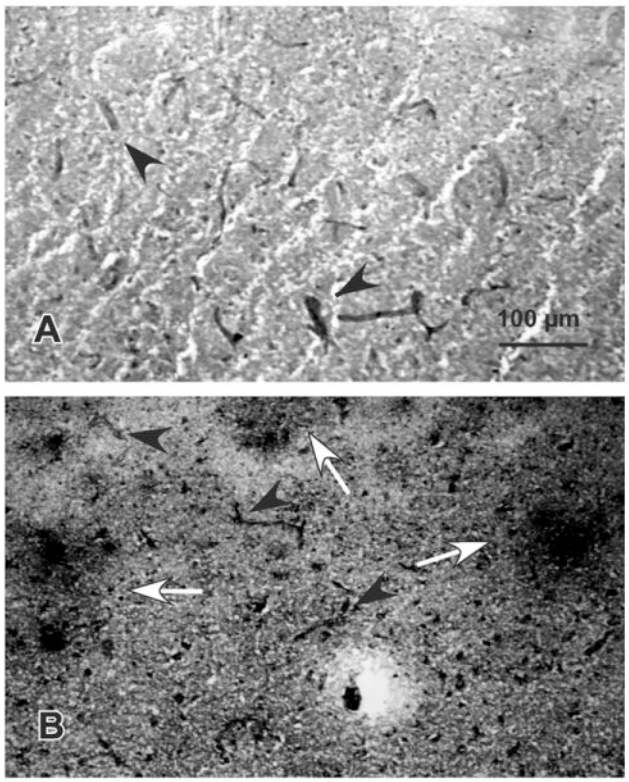

Fig. 3.

Micrographs of immunostaining with the mouse monoclonal antibody to ICAM-1 in cortical area 47. The top picture is from a 60-year-old female and the bottom picture is from as 86-year-old female. Arrowheads in both pictures point to ICAM-1-IR structures with vascular morphology. Arrows in the bottom picture denote patches of ICAM-1-I. These patches were mostly absent in the subject at the top. Calibration bar, 100 μm.

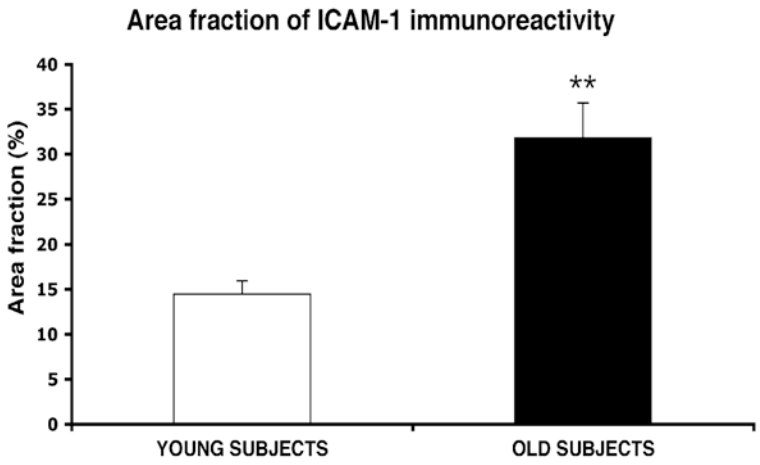

Fig. 4.

Bar graphs representing the area fraction of all (vascular + extravascular) ICAM-1-IR structures combined in subjects less than 60 years old at the time of death (young) and subjects older than 60 (old). $^{**}p < .0001$.

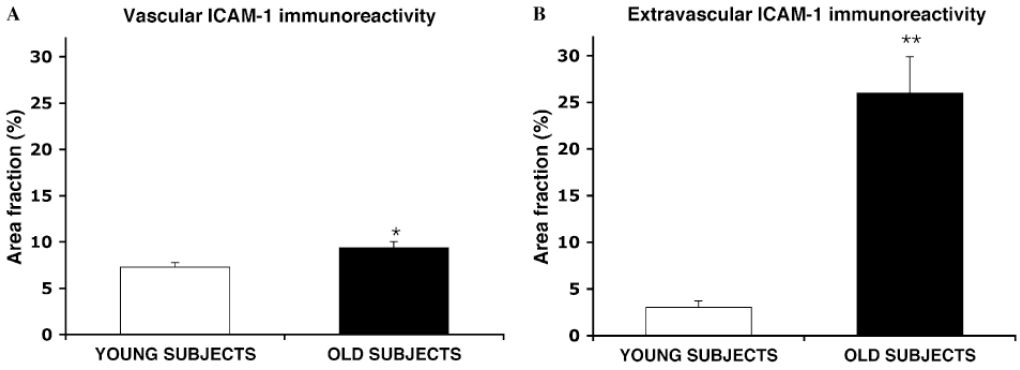

Fig. 5.

Bar graphs representing the area fraction of ICAM-1 immunoreactivity in structures with vascular morphology (vessels) (A) and in extravascular patches of ICAM-1 immunoreactivity (B). *X* axis legends as in Fig. 3. *$p < .01$, **$p < .00001$.

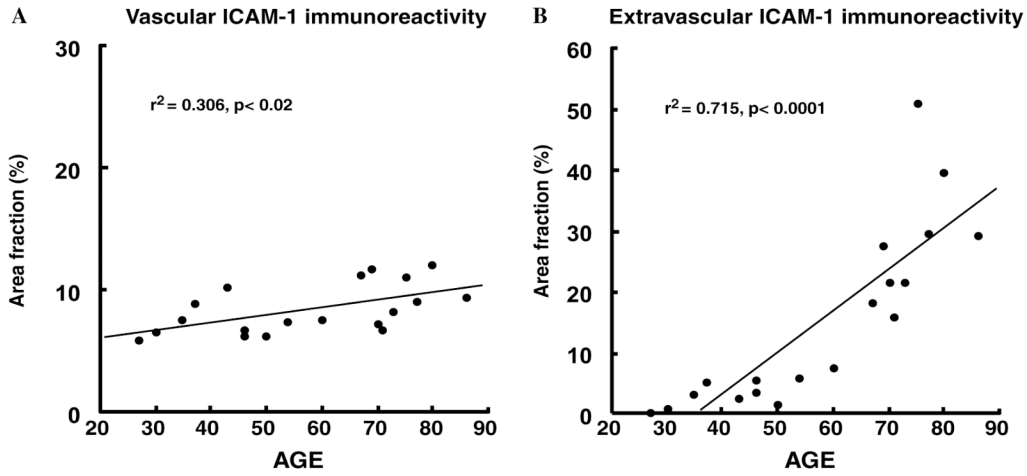

Fig. 6.

Plots of the values of the area fraction of ICAM-1-I in the vascular (A) and extravascular (B) compartments according to the age of the all subjects combined. A significant correlation of both vascular and extravascular ICAM-1-I with age was detected. The correlation is much steeper for extravascular ICAM-1-I than for vascular ICAM-1-I.

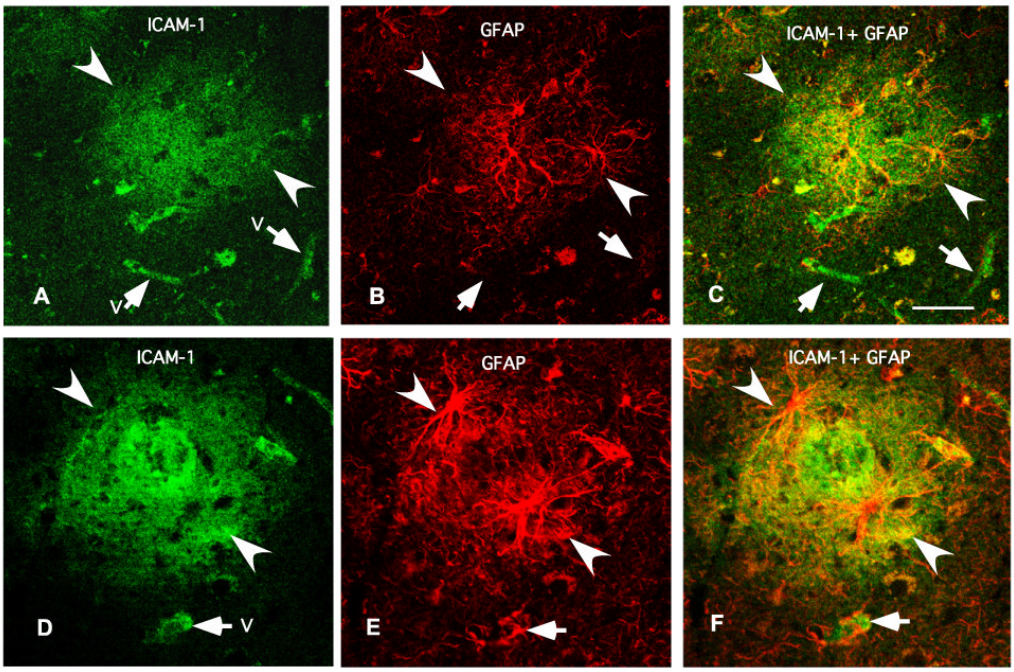

Fig. 7.

Micrographs of two typical arrangements (top and bottom) of ICAM-1 immunoreactivity in relation to GFAP-IR astrocytes obtained using simultaneously antibodies to ICAM-1 and the astrocytic marker GFAP in a 73 years old subject. Note in (C) and (F) (yellow spots) that the patches of diffuse ICAM-1 immunoreactivity (in green in (A) and (C)) are confined within the area affected by GFAP-IR processes (in red in (B) and (E)). ICAM-1 immunoreactivity is also observable in vessels ("v" and arrows). Calibration bar is 50 μm.

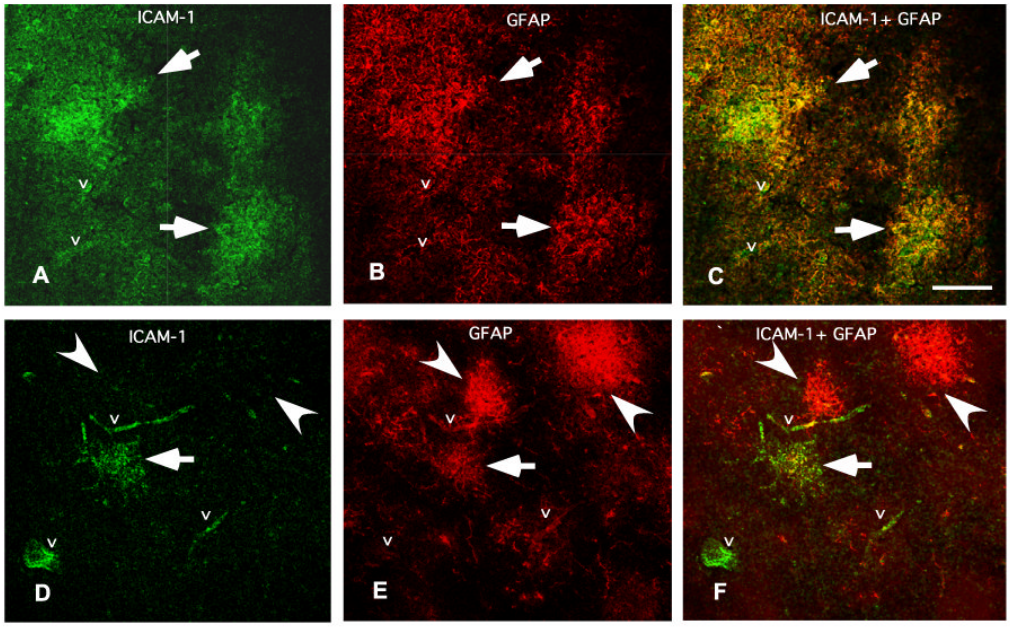

Fig. 8.

Comparison of co-labeling for ICAM-I and GFAP in an 86 years old subject (A, B and C) and in a 27 years old subject (D, E and F). Note that in the old subject all GFAP positive structures are co-extensive with ICAM-1-IR patches (C). By contrast, in the younger subject only one of the GFAP-IR astrocytes is in register with ICAM-1 immunoreactivity (F). The letter “v” designates ICAM-1 immunoreactivity in vessels. Arrows indicate ICAM-1 immunoreactivity (green) in register with GFAP immunoreactive structures (red). Calibration bar is 100 μm.

Table 1

Characteristics of subjects included in the present study

Subject	Age (years)	PMD (hours)	Gender	Race	Cause of death
1	27	15	F	C	Hypertensive cardiovascular disease
2	30	19	M	AA	Hypertrophic cardiomyopathy
3	35	25	M	C	Heart disease
4	37	13	F	C	Viral myocarditis
5	43	23	M	C	Pulmonary thromboembolism
6	46	24	F	C	Homicide
7	46	11	M	AA	Heart disease
8	50	27	F	C	Heart complications
9	54	29	M	C	Myocardial infarct
10	60	19	F	AA	Aortic aneurism
11	67	24	M	C	Atherosclerotic cardiovascular disease
12	69	18	M	C	Heart-dissecting aortic aneurism
13	70	20	M	C	Heart problems
14	71	24	M	C	Myocardial infarct, cardiac rupture
15	73	24	M	AA	Heart disease
16	75	32	F	C	Myocardial infarct
17	77	24	M	C	Heart disease
18	80	21	F	C	Hypertensive sclerotic heart disease with remote myocardial infarct
19	86	18	F	C	Coronary sclerotic heart disease with myocardial fibrosis and cardiomegaly

Abbreviations: AA, African-American; C, Caucasian; F, female; M, male; PMD, postmortem delay (time between death and freezing of brain samples).